Chapter 4 - Bulk Metallic Glass with Benchmark Thermoplastic Processability

After discovering the large ΔT alloys discussed in Chapter 3, we characterized the most promising of them to determine if we had made any improvements over other alloys used for thermoplastic forming (TPF). Two alloys were studied in parallel and are reported in this chapter. The data for the alloys is considered nearly interchangeable because of the similarity of compositions. The two compositions are $Zr_{35}Ti_{30}Cu_{8.25}Be_{26.75}$ (ΔT = 159 K) and $Zr_{35}Ti_{30}Cu_{7.5}Be_{27.5}$ (ΔT = 165 K). This chapter is based on a talk given at the MRS conference in Boston 2007 and an article entitled "Bulk Metallic Glass with Benchmark Thermoplastic Processability" [G. Duan, A. Wiest, M.L. Lind, J. Li, W.K. Rhim, and W.L. Johnson, Adv. Mater. 19 (2007) 4272] The article can be found at DOI: 10.1002/adma.200700969. The text has been changed in many places to reflect recent research and should be compared to the original document if all changes are of interest.

The exceptional processability and large supercooled liquid region (SCLR) of bulk amorphous metals makes them highly promising candidates for thermoplastic processing. We report a lightweight (ρ = 5.4 g/cm^3) quaternary glass forming alloy, $Zr_{35}Ti_{30}Cu_{8.25}Be_{26.75}$, having the largest supercooled liquid region, ΔT = 159 K (at 20 K/min heating rate) of any known bulk glass forming alloy. The alloy can be cast into fully amorphous rods of diameter = 1.5cm. The undercooled liquid exhibits an unexpectedly high Angell Fragility of m = 65.6. Based on these features, it is demonstrated that this alloy exhibits "benchmark" characteristics for thermoplastic processing. We report results of mechanical, thermal, rheological, and time temperature transformation (TTT) studies on this new material. The alloy exhibits high yield strength and excellent fracture toughness, and a relatively high Poisson's ratio. Simple

microreplication experiments carried out in open air using relatively low applied pressures demonstrate superior thermoplastic processability for engineering applications. Chapter 5 will demonstrate a modified injection molding setup that allowed TPF with high strains.

Over the last two decades, the unique properties of bulk metallic glasses (BMG), such as high strength, high specific strength, large elastic strain limit, and excellent wear and corrosion resistances along with other remarkable engineering properties have made these materials of significant interest for science and industry [1-9]. Researchers have designed families of multi-component systems that form bulk amorphous alloys [4–9], among which Zr based (Vitreloy series) [4], and Pt based [8] BMG have been utilized commercially to produce items including sporting goods, electronic casings, medical devices, and fine jewelries.

The unique advantages of injection molding, blow molding, microreplication, and other thermoplastic technologies are largely responsible for the widespread uses of plastics such as polyethylene, polyurethane, PVC, etc., in a broad range of engineering applications. Powder injection molding of metals represents an effort to apply similar processing to metals, but requires blending of the powder with a plastic binder to achieve net shape forming and subsequent sintering of the powder. Given suitable materials, thermoplastic forming (TPF) would be the method of choice for manufacturing of net shape metallic glass components because TPF decouples the forming and cooling steps by processing glassy material at temperatures above the glass transition temperature (T_g) and below the crystallization temperature (T_x) followed by cooling to ambient temperature [10-11]. Conventional die casting requires rapid quenching to bypass the

crystallization nose, which limits the ability to make high quality casts and to create parts with complex geometries. Unfortunately, among the published metallic glasses none of the alloys used in TPF processes to date reach viscosities suitable to mimic polymer plastics formability with sufficient time to use conventional plastic processing techniques. Alloys in the expensive Pt and Pd based [8, 12-13] families have shown good thermoplastic formability reaching viscosities of around 10^5 Pa-s with sufficient time available for processing. Zr based metallic glasses are much less expensive than Pt and Pd based alloys. Unfortunately, Zr based BMG forming alloys have low fragilities, and low processing viscosities are only attainable in the SCLR [14-15] with alloys having large ΔT. Strain rate effects on viscosity of amorphous alloys have been extensively studied [16-17].

An alloy optimal for TPF should have good glass forming ability, low viscosity / high fragility in the SCLR, a low processing temperature, and a long processing time at that temperature before crystallization. We studied Be bearing ZrTi based quaternary metallic glasses with compositions in the range of $60\% \leq Zr + Ti \leq 70\%$. We found that compared with Vitreloy alloys $(Zr + Ti = 55\%)$, T_g is lowered, the liquid appears to become more fragile, and the SCLR is increased. The apparent increase in fragility may be due to two phase flow effects that are further discussed in Chapter 6. Two composition regions were found with alloys that exhibit exceptional properties for TPF in the $Zr_a Ti_b Cu_c Be_d$ system. These were $a \approx b$ with $c \leq 12.5\%$, and $a \approx 5b$ with $d \geq 20\%$. DSC curves of three representative alloys are presented in Figure 4.1. The alloys all exhibit a very large SCLR with a single sharp crystallization peak at which the alloy undergoes massive crystallization to a multiphase crystalline product.
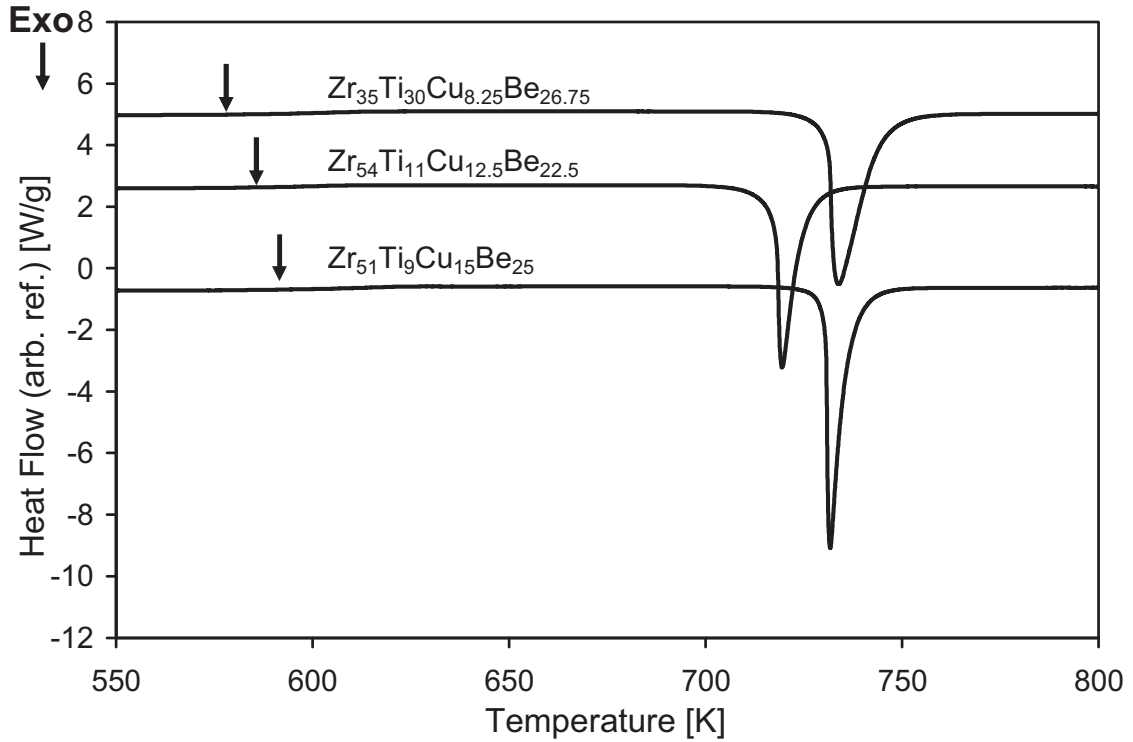
Figure 4.1: DSC scans of three typical bulk metallic glasses with excellent glass forming ability and extremely high thermal stability. The marked arrows represent the glass transition temperatures.

The 5 gram samples were generally found to freeze without any crystallization during preparation resulting in a glassy ingot. The $Zr_{35}Ti_{30}Cu_{8.25}Be_{26.75}$ alloy can be cast into fully amorphous rods of diameter = 1.5cm. The amorphous nature of all the samples studied in this work has been confirmed by X-ray diffraction. A summary of thermal properties of these BMG is listed in Table 4.1 and compared with several earlier reported amorphous alloys.[4, 7-8, 12, 18–21] The variations of SCLR, ΔT ($\Delta T = T_x - T_g$, in which T_x is the onset temperature of the first crystallization event), and reduced glass transition temperature T_{rg} ($T_{rg} = T_g/T_L$, where T_L is the liquidus temperature) are calculated. In the three newly designed alloys, $Zr_{35}Ti_{30}Cu_{8.25}Be_{26.75}$ exhibits the lowest T_g (578 K and about 45 K lower than that of Vitreloy 1 or Vitreloy 4) and the largest ΔT

(159 K). It was further found that ΔT of the same glass can be enlarged to be 165 K by addition of 0.5% Sn, giving the largest SCLR reported for any known bulk metallic glass.

Table 4.1: Thermal, mechanical, and rheological properties of various BMG forming alloys.

Material	T_g [K]	T_x [K]	T_L [K]	ΔT [K]	T_{rg} [K]	m	s	$m^*\Delta T^*_{rx}$	G [Gpa]	Y [Gpa]	υ
$Zr_{51}Ti_9Cu_{15}Be_{25}$	592	730	1047	138	0.565	-	0.30	-	31.8	86.5	0.36
$Zr_{54}Ti_{11}Cu_{12.5}Be_{22.5}$	581	721	1035	140	0.561	-	0.31	-	30.3	82.8	0.37
$Zr_{35}Ti_{30}Cu_{8.25}Be_{26.75}$	578	737	1044	159	0.554	65.6	0.34	20.3	31.8	86.9	0.37
$Zr_{41.2}Ti_{13.8}Ni_{10}Cu_{12.5}Be_{22.5}$	623	712	993	89	0.627	49.9	0.24	8.0	37.4	101.3	0.35
$Zr_{46.75}Ti_{8.25}Ni_{10}Cu_{7.5}Be_{27.5}$	625	738	1185	113	0.527	44.2	0.20	10.0	35.0	95.0	0.35
$Pd_{43}Ni_{10}Cu_{27}P_{20}$	575	665	866	90	0.664	58.5	0.31	12.3	33.0	92.0	0.39
$Pt_{60}Ni_{15}P_{25}$	488	550	804	60	0.596	67.2	0.17	12.5	33.8	96.1	0.42
$Ce_{68}Cu_{20}Al_{10}Nb_2$	341	422	643	81	0.530	-	0.26	-	11.5	30.3	0.31
$Au_{49}Ag_{5.5}Pd_{2.3}Cu_{26.9}Si_{16.3}$	401	459	644	58	0.623	-	0.24	-	26.5	74.4	0.41
$Pt_{57.5}Ni_{5.3}Cu_{14.7}P_{22.5}$	508	606	795	98	0.639	-	0.34	-	33.4	95.7	0.43

In Figure 4.2, the temperature dependence of equilibrium Newtonian viscosity of $Zr_{35}Ti_{30}Cu_{8.25}Be_{26.75}$ and several other metallic glass forming liquids with different Angell fragility numbers [22] are presented. The solid curve represents a Vogel-Fulcher-Tammann (VFT) fit to the viscosity data of $Zr_{35}Ti_{30}Cu_{8.25}Be_{26.75}$:

$$\eta = \eta_0 \exp\left(\frac{D^* * T_0}{T - T_0}\right)$$

where η_0, D^*, and T_0 are fitting constants. T_0 is the VFT temperature and $\eta_0 \approx 10^{-5}$ Pa-s. In the best fit, $T_0 = 422.6$ K and $D^* = 12.4$ are found, which yields an Angell fragility number of m = 65.6. This high fragility value could be a result of the two T_g relaxation phenomenon that will be presented in Chapter 6. No viscosity data near T_g was collected so the VFT fit used to calculate fragility, which is the slope of the Log[$\eta(T/T_g)$] curve at T_g (see Derivation 5), may be off. The fragility calculated from the VFT fit is quite high

when compared to fragilities for other Vitreloy glasses which are typically in the range of

m = 30 - 40 [23]. If we fit the data using the viscosity formula based on metallic glass

physics proposed by Johnson [23] and detailed in Derivation 5 we find that m = 40 and

T_g = 539 K. The value for T_g calculated using the Johnson formula is close to the T_g

measured at 20 K/min in the DSC = 578 K and the fragility is more in line with what

would be expected for a Vitreloy type alloy.
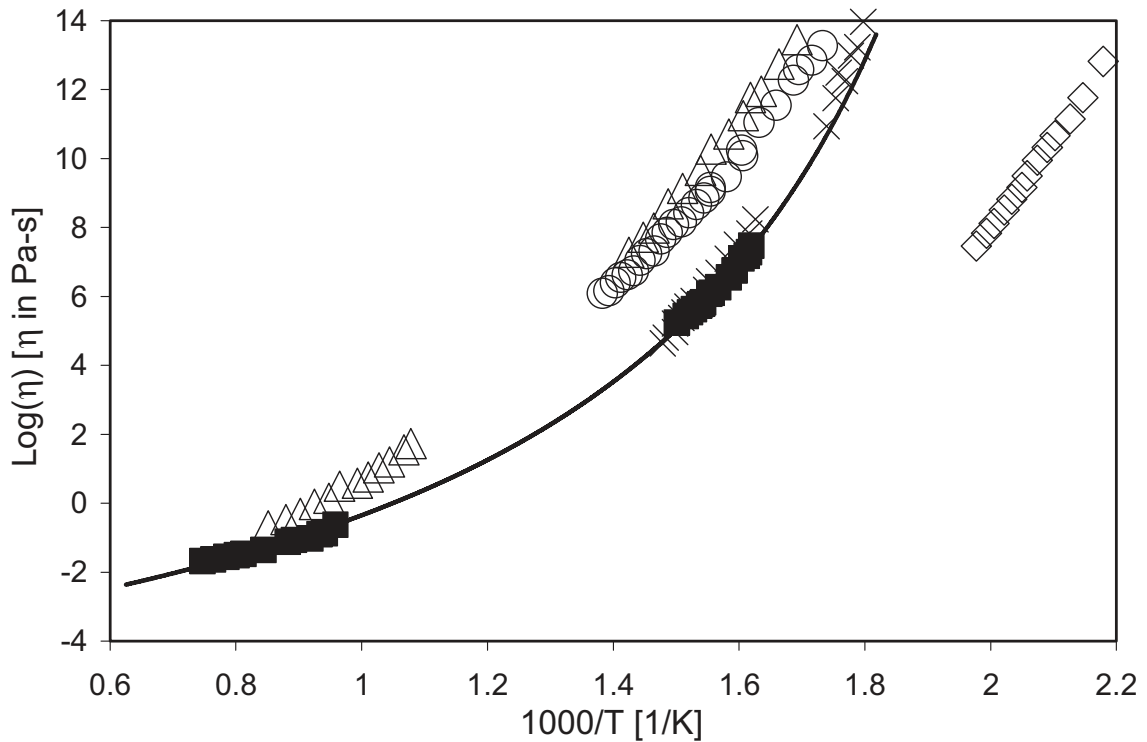
Figure 4.2: The temperature dependence of equilibrium viscosity of several metallic glass forming liquids: $Zr_{41.2}Ti_{13.8}Ni_{10}Cu_{12.5}Be_{22.5}$ (Vitreloy 1) ($\triangle$); $Zr_{46.25}Ti_{8.25}Cu_{7.5}Ni_{10}Be_{27.5}$ (Vitreloy 4) ($\circ$); $Zr_{35}Ti_{30}Cu_{8.25}Be_{26.75}$ ($\blacksquare$); $Pd_{43}Ni_{10}Cu_{27}P_{20}$ ($\times$); $Pt_{60}Ni_{15}P_{25}$ ($\lozenge$). It is shown that the viscosity of $Zr_{35}Ti_{30}Cu_{8.25}Be_{26.75}$ in the thermoplastic processing region is at least two orders of magnitude lower than that of Vitreloy 1 or Vitreloy 4 and is comparable to that of Pd based metallic glass and polymer glasses.

The Angell fragility parameters of Vitreloy series, Pd based, and Pt based metallic

glass forming liquids [19, 24-25] are listed in Table 4.1 as well. $Zr_{35}Ti_{30}Cu_{8.25}Be_{26.75}$

shows rather fragile behavior compared with the strong Vitreloy series of liquids. Its

viscosity in the thermoplastic zone is at least two orders of magnitude lower than that of

Vitreloy 1 or Vitreloy 4 at the same temperature and is comparable to that of Pd based metallic glass. For example, the equilibrium viscosity at 683 K for $Zr_{35}Ti_{30}Cu_{8.25}Be_{26.75}$ is measured to be only $8*10^4$ Pa-s, similar to that of viscous polymer melts [26]. As is known from the processing of thermoplastics, the formability is inversely proportional to viscosity. This alloy's low viscosity in the SCLR will result in a low Newtonian flow stress and high formability.

Recently, the normalized thermal stability, S, which is defined as $\Delta T/(T_L - T_g)$, was introduced to characterize the thermoplastic formability [10]. As indicated in Table 4.1, $Zr_{35}Ti_{30}Cu_{8.25}Be_{26.75}$ demonstrates an S value of 0.34, which is higher than that of all the other alloys and is as good as $Pt_{57.5}Cu_{14.7}Ni_{5.3}P_{22.5}$. Because the S parameter is based on an oversimplified assumption of identical viscosity at T_L, a deformability parameter,

$d^* = Log[\eta(T_g^*)/\eta(T_x)]$ [19] was also proposed and correlated with Angell fragility (m)

and the reduced thermal stability, $\Delta T_{rx}^* = (T_x - T_g^*)/T_g^*$, where T_g^* is the glass transition temperature at which the viscosity is 10^{12} Pa-s. Table 4.1 lists the calculated $m*\Delta T_{rx}^*$ values for $Zr_{35}Ti_{30}Cu_{8.25}Be_{26.75}$, Vitreloy 1, Vitreloy 4, $Pd_{43}Ni_{10}Cu_{27}P_{20}$, and $Pt_{60}Ni_{15}P_{25}$ based on the measured viscosity data. It is seen clearly that $Zr_{35}Ti_{30}Cu_{8.25}Be_{26.75}$ shows the largest $m*\Delta T_{rx}^*$, which implies a superior thermoplastic workability.

In Figure 4.3, we present the measured TTT curve for $Zr_{35}Ti_{30}Cu_{8.25}Be_{26.75}$ and other Vitreloy series alloys [27]. The TTT curve indicates a nose shape, with the minimum crystallization time of about 3 - 10 s occurring somewhere between 700 K and 950 K. The data on the bottom part of the nose was collected by heating the metallic glass from room temperature. The data on the top part of the nose was obtained by cooling the material from the melt. Because of insufficient GFA, the bottom part of the

cooling TTT curve was inaccessible with the cooling rates available to us. Both sets of data are shown on the same graph for convenience. At 683 K, where the equilibrium viscosity is about $8*10^4$ Pa-s, a 600 s thermoplastic processing window is available for forming.
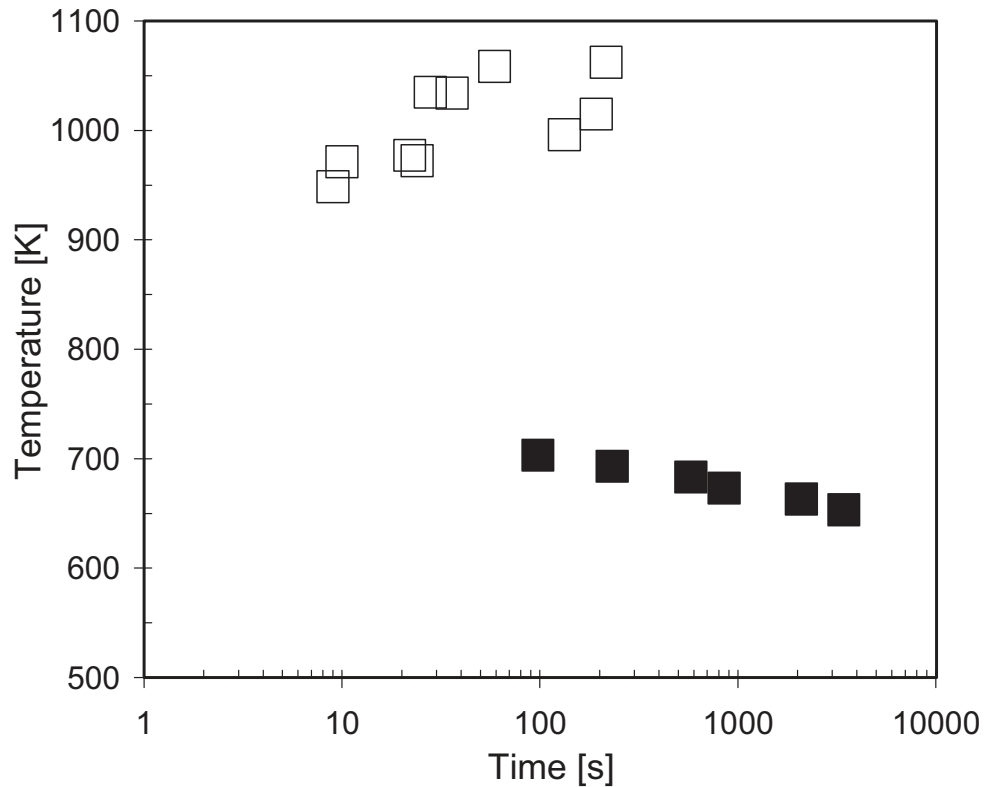
Figure 4.3: TTT diagrams for $Zr_{35}Ti_{30}Cu_{8.25}Be_{26.75}$ upon heating (■), and cooling (□). The data were measured by electrostatic levitation for cooling measurements. TTT upon heating measurements were done by processing in graphite crucibles after heating from the amorphous state. At 683 K, where the equilibrium viscosity is about $8*10^4$ Pa-s, a 600 s thermoplastic processing window is available.

To demonstrate the strong thermoplastic processability of the $Zr_{35}Ti_{30}Cu_{8.25}Be_{26.75}$ glassy alloy, we carried out plastic forming experiments as shown in Figure 4.4. The thermoplastic processing was done on a Tetrahedron hot press machine in air at a pressure of 25 MPa with a processing time of 45 s, followed by a water quenching step. Figure 4.4 shows the microformed impression of a United States dime (Figure 4.4b) made on TPF metallic glass ingots at about 643 K (Figure 4.4a). Minimal oxidation was

observed after processing, which is consistent with the strong oxidation resistance of Be

bearing amorphous alloys. The final parts remain fully amorphous as verified by X-ray

diffraction. It is found from the Rockwell hardness tests that no degradation of the

mechanical properties was caused by the thermoplastic processing. Before the TPF was

carried out, we produced diamond shaped microindentation patterns (~ 100μm) in the top

flame of the dime using a Vickers hardness tester (Figure 4.4c). Figure 4.4d presents the

successfully replicated diamond pattern in the final part. Even the scratches (on the level

of several μm) on the original dime are clearly reproduced. Although the induced strain

was small, replication of small features is shown.
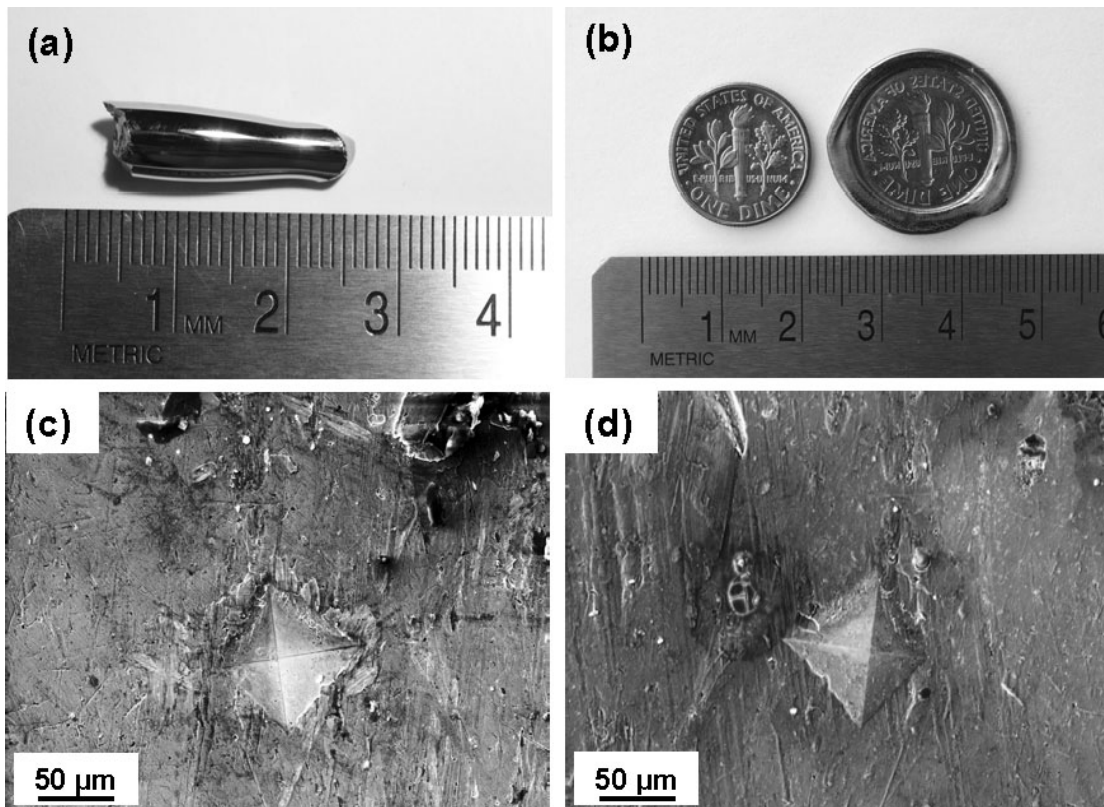
Figure 4.4: Demonstration of the strong thermoplastic processability of the $Zr_{35}Ti_{30}Cu_{8.25}Be_{26.75}$ metallic glass. The ingot in (a) is pressed over a dime at 643 K for 45 s at 25 MPa to form the negative imprint of a United States dime shown in (b). A diamond shaped microindentation pattern was placed in the flame on the dime (c) and was successfully replicated in the negative imprint (d) as well.

The imprinting and microreplication test on the dime required minimal thermoplastic strain. However, many TPF processes like injection molding require large strains to move material from a reservoir to a mold cavity. We used a method proposed by Schroers [28] to compare glassy alloys commonly used in TPF processes with the newly developed large ΔT alloy for TPF processes requiring large strains. The method proposed by Schroers involves applying a constant force to a known volume of each alloy through the SCLR at a constant heating rate. We chose a force of 2000 lbs, 10 K/min heating rate, and 0.1cm^3 of each alloy. The alloys of interest were $Pd_{43}Ni_{10}Cu_{27}P_{20}$, $Pt_{57.5}Ni_{5.3}Cu_{14.7}P_{22.5}$, $Zr_{41.2}Ti_{13.8}Cu_{12.5}Ni_{10}Be_{22.5}$ (Vitreloy 1), and $Zr_{44}Ti_{11}Cu_{10}Ni_{10}Be_{25}$ (Vitreloy 1b). Schroers squish test is depicted in Figure 4.5 along with pictures of the squished alloys and a table of the results.
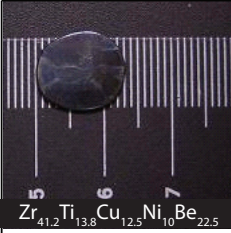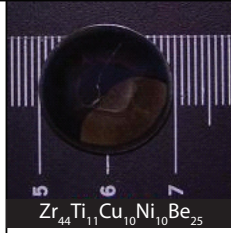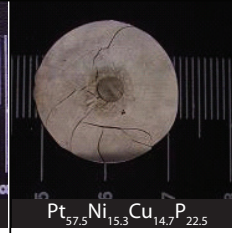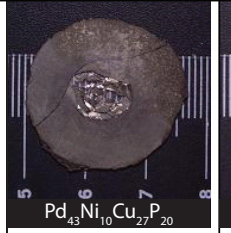
Formability Characterization

2000 lb
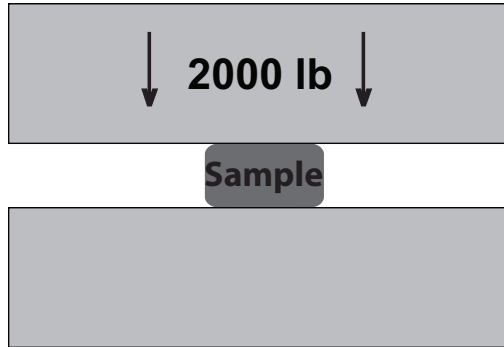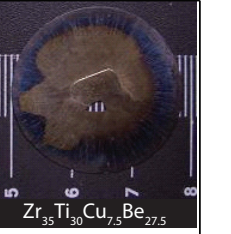
Sample

Process in entire ΔT region
$T_g < T < T^x$

dT/dt = 10 K/min
Sample size= 0.1 cm^3
Final Diameter indicates
thermoplastic formability

$Zr_{41.2}Ti_{13.8}Cu_{12.5}Ni_{10}Be_{22.5}$	$Zr_{44}Ti_{11}Cu_{10}Ni_{10}Be_{25}$	$Pt_{57.5}Ni_{15.3}Cu_{14.7}P_{22.5}$	$Pd_{43}Ni_{10}Cu_{27}P_{20}$	$Zr_{35}Ti_{30}Cu_{7.5}Be_{27.5}$
Diam = 12.8mm	21.7mm	23.7mm	24.7mm	28.5mm
Tg = 620.2 K	619.4 K	499.3 K	575.6 K	578 K
Tx = 681.1 K	760.3 K	577.0 K	676.5 K	743 K
Fragility = 40	35	59	58	40 or 65.6

Figure 4.5: Squish test proposed by Schroers [28] performed on four alloys traditionally used in TPF and the new large ΔT alloy. The largest diameter after the squish test is obtained by using the $Zr_{35}Ti_{30}Cu_{7.5}Be_{27.5}$ alloy suggesting that it will exhibit the best flow properties in TPF processes requiring large strains.

The elastic constants of $Zr_{35}Ti_{30}Cu_{8.25}Be_{26.75}$ and several other BMG are also shown in Table 4.1. Evidence suggests that a high Poisson's ratio is related to the ductile behavior of metallic glasses [29-34]. $Zr_{35}Ti_{30}Cu_{8.25}Be_{26.75}$ has a Poisson's ratio of ~ 0.37, higher than that of Vitreloy series alloys. The fracture toughness (K_{1C}) of $Zr_{35}Ti_{30}Cu_{8.25}Be_{26.75}$ was estimated to be ~ 85 MPa m$^{1/2}$, while that of Vitreloy 1 is only ~ 20 – 45 MPa m$^{1/2}$ [35–37]. The yield strength of $Zr_{35}Ti_{30}Cu_{8.25}Be_{26.75}$ under uniaxial compressive tests was found to be ~ 1.43 GPa. To design this new class of BMG, a balance between strength and thermoplastic processability has to be obtained [38]. The

present series of amorphous metals possesses superior thermoplastic formability with a minimum reduction of yield strength and elastic energy storage.

In summary, we have designed a series of metallic glass forming alloys, having the combination of optimized properties for TPF, such as extraordinarily low viscosity in the thermoplastic zone, exceptional thermal stability, low T_g, and excellent GFA. These alloys demonstrate strong thermoplastic processability and excellent mechanical properties. We expect that this discovery will greatly broaden the engineering applications of amorphous metals by taking advantage of the unique properties of the newly designed BMG.

4.1 Experimental Method

Mixtures of elements of purity ranging from 99.9% to 99.99% were alloyed by induction melting on a water cooled silver boat under a Ti-gettered argon atmosphere. Typically 5 g ingots were prepared. Each ingot was flipped over and remelted at least three times in order to obtain chemical homogeneity. A Philips X'Pert Pro X-ray Diffractometer and a Netzsch 404C Pegasus Differential Scanning Calorimeter (DSC performed at a constant heating rate 0.33 K/s) were utilized to confirm the amorphous natures and to examine the isothermal behaviors in the SCLR of these alloys. The pulse-echo overlap technique with 25 MHz piezoelectric transducers was used to measure the shear and longitudinal wave speeds at room temperature for each of the samples. Sample density was measured by the Archimedean technique according to the American Society of Testing Materials standard C 693-93 [39]. The viscosity of $Zr_{35}Ti_{30}Cu_{8.25}Be_{26.75}$ as a function of temperature in the SCLR was studied using a Perkin Elmer TMA7 Thermomechanical Analyzer (TMA) in the parallel plate geometry as described by

Bakke, Busch, and Johnson [40]. The measurement was done with a heating rate of 0.667 K/s, a force of 0.02 N, and an initial height of 0.3mm. The viscosity and TTT diagrams of $Zr_{35}Ti_{30}Cu_{8.25}Be_{26.75}$ at high temperatures were measured in a high vacuum electrostatic levitator (ESL) [41-42]. For the viscosity measurements, the resonant oscillation of the molten drop was induced by an alternating current electric field while holding the sample at a preset temperature. Viscosity was calculated from the decay time constant of free oscillation that followed the excitation pulse. To determine the TTT curve, an electrostatically levitated molten (laser melting) droplet (~ 3mm diameter) sample was cooled radiatively to a predetermined temperature, and then held isothermally until crystallization. The temperature fluctuations were within ± 2 K during the isothermal treatment.

Chapter 4 References

[1]   A.L. Greer, Science 267 (1995) 1947.
[2]   W.L. Johnson, MRS Bull. 24 (1999) 42.
[3]   A. Inoue, Acta Mater. 48 (2000) 279.
[4]   A. Peker, W.L. Johnson, Appl. Phys. Lett. 63 (1993) 2342.
[5]   D.H. Xu, G. Duan, W.L. Johnson, Phys. Rev. Lett. 92 (2004) 245504.
[6]   V. Ponnambalam, S.J. Poon, G.J. Shiflet, J. Mater. Res. 19 (2004) 1320.
[7]   B. Zhang, D.Q. Zhao, M.X. Pan, W.H. Wang, A.L. Greer, Phys. Rev. Lett. 94 (2005) 205502.
[8]   J. Schroers, W.L. Johnson, Appl. Phys. Lett. 84 (2004) 3666.

[9]   Z.P. Lu, C.T. Liu, J.R. Thompson, W.D. Porter, Phys. Rev. Lett. 92 (2004) 245503.
[10]   J. Schroers, JOM 57 (2005) 35.
[11]   J. Schroers, N. Paton, Adv. Mater. Proc. 164 (2006) 61.
[12]   G.J. Fan, H.J. Fecht, E.J. Lavernia, Appl. Phys. Lett. 84 (2004) 487.
[13]   J.P. Chu, H. Wijaya, C.W. Wu, T.R. Tsai, C.S. Wei, T.G. Nieh, J. Wadsworth, Appl. Phys. Lett. 90 (2007) 034101.
[14]   A. Masuhr, T.A. Waniuk, R. Busch, W.L. Johnson, Phys. Rev. Lett. 82 (1999) 2290.
[15]   R. Busch, W.L. Johnson, Appl. Phys. Lett. 72 (1998) 2695.
[16]   F. Spaepen, Acta Metall. 25 (1977) 407.
[17]   J. Lu, G. Ravichandran, W.L. Johnson, Acta Mater. 51 (2003) 3429.
[18]   T.A. Waniuk, J. Schroers, W.L. Johnson, Appl. Phys. Lett. 78 (2001) 1213.
[19]   H. Kato, T. Wada, M. Hasegawa, J. Saida, A. Inoue, H.S. Chen, Scripta Mater. 54 (2006) 2023.
[20]   K. Shibata, T. Higuchi, A.P. Tsai, M. Imai, K. Suzuki, Prog. Theor. Phys. Suppl. 126 (1997) 75.
[21]   J. Schroers, B. Lohwongwatana, W.L. Johnson, A. Peker, Appl. Phys. Lett. 87 (2005) 061912.
[22]   L.M. Martinez, C.A. Angell, Nature 410 (2001) 663.
[23]   W.L. Johnson, M.D. Demetriou, J.S. Harmon, M.L. Lind, K. Samwer, MRS Bull. 32 (2007) 644.
[24]   V.N. Novikov, A.P. Sokolov, Phys. Rev. B 74 (2006) 064203.
[25]   D.N. Perera, J. Phys. Condens. Matter 11 (1999) 3807.
[26]   F.W. Billmeyer, Text. Ploym. Sci. (1984) 305.
[27]   T. Waniuk, J. Schroers, W.L. Johnson, Phys. Rev. B 67 (2003) 184203.
[28]   J. Schroers, Acta Mater. 56 (2008) 471.
[29]   H.S. Chen, J.T. Krause, E. Coleman, J. Non-Cryst. Solids 18 (1975) 157.
[30]   V.N. Novikov, A.P. Sokolov, Nature 431 (2004) 961.
[31]   J. Schroers, W.L. Johnson, Phys. Rev. Lett. 93 (2004) 255506.
[32]   W.L. Johnson, K. Samwer, Phys. Rev. Lett. 95 (2005) 195501.
[33]   X.J. Gu, A.G. McDermott, S.J. Poon, G.J. Shiflet, Appl. Phys. Lett. 88 (2006) 211905.
[34]   J.J. Lewandowski, W.H. Wang, A.L. Greer, Philos. Mag. Lett. 85 (2005) 77.
[35]   J.J. Lewandowski, M. Shazly, A.S. Nouri, Scripta Mater. 54 (2006) 337.
[36]   P. Lowhaphandu, J.J. Lewandowski, Scripta Mater. 38 (1998) 1811.
[37]   J.J. Lewandowski, Mater. Trans. 42 (2001) 633.
[38]   G. Duan, M.L. Lind, K. De Blauwe, A. Wiest, W.L. Johnson, Appl. Phys. Lett. 90 (2007) 211901.
[39]   M.L. Lind, G. Duan, W.L. Johnson, Phys. Rev. Lett. 97 (2006) 015501.
[40]   E. Bakke, R. Busch, W.L. Johnson, Appl. Phys. Lett. 67 (1995) 3260.
[41]   S. Mukherjee, J. Schroers, Z. Zhou, W.L. Johnson, W.K. Rhim, Acta Mater. 52 (2004) 3689.
[42]   S. Mukherjee, Z. Zhou, J. Schroers, W.L. Johnson, W.K. Rhim, Appl. Phys. Lett. 84 (2004) 5010.